

Diffraction of sound by a rigid screen

with a soft or perfectly absorbing edge

A.D. Rawlins

Department of Mathematics,

The University,

Dundee,

DD1 4HN

Scotland.

A B S T R A C T

A solution is obtained for the problem of the diffraction of a plane wave sound source by a semi-infinite plane. A finite region in the vicinity of the edge has a soft (pressure release) boundary condition; the remaining part of the semi-infinite plane is rigid.

This solution is then used to derive an approximation for the behaviour of a rigid barrier with an absorbing edge. It is concluded that the absorbing material that comprises the edge need only be of the order of a wavelength long to have approximately the same effect, on the sound attenuation in the shadow side of the barrier, as a completely absorbent barrier.

Introduction

In recent years noise reduction by barriers has become a common measure of environmental protection in heavily built-up areas.

In particular, noise from motorways, railways and airports can be shielded by a barrier which intercepts the line-of-sight from the source to the receiver. The acoustic field in the shadow region of a barrier, (when transmission through the barrier is negligible) is due to diffraction at the edge alone.

The design of such noise barriers should meet two important requirements, namely, that they are effective noise attenuators, and that their construction and maintenance should be economical. The latter requirement is not difficult to appreciate when one considers the miles of motorway which runs through built-up areas. One possible economic barrier construction is to have a rigid barrier (hence reducing transmitted noise) of cheap material which is robust, and not necessarily a good attenuator of edge diffracted noise, and to cover the surfaces of the barrier with a sound absorbing lining which is a good attenuator of sound. The provision of a barrier covered completely with an absorbing lining presents several difficulties among them the cost of construction and maintenance. However, since diffraction phenomena are governed by conditions at the diffracting edge, it would be more economic to cover the region only in the immediate vicinity of the edge with sound absorbing material^{see Butler [1]}. A question of some importance therefore is: what length of absorbing material would be required to obtain approximately the same noise attenuation as a completely absorbent barrier? It is hoped that the present theoretical work will help to answer this question.

The presence of an acoustically absorbing lining on a surface is

usually described by an impedance relation between the pressure (p) and the normal velocity fluctuation on the lining surface, see Morse and Ingard [2]. This gives rise to a boundary condition on the absorbing lining of the form

$$\frac{\partial p}{\partial n} = ik\beta p, \quad \text{Re}(\beta) > 0,$$

where the sound wave has time harmonic variation $e^{-i\omega t}$ and

$k = \omega/c$, c is the velocity of sound, n the normal pointing into the lining, and β the complex specific admittance of the acoustic lining (see Rawlins [3]). An acoustically hard (or perfectly reflecting) surface has a vanishing admittance i.e. $|\beta| \rightarrow 0$

and an acoustically soft surface (pressure fluctuation vanishing on surface) is given by $|\beta| \rightarrow \infty$. The limiting case when the edge region of the barrier surface is soft is considered and the solution to this problem gives, by simple superposition, the solution to the problem of a rigid barrier with a perfectly absorbing edge.

[INSERT PAGES 3A and 3b HERE]

If the wavelength of the sound is much smaller than the length scale associated with the barrier, the diffraction process is governed to all intents and purposes by the solution to the canonical problem of diffraction by a semi-infinite half-plane.

Under the above approximations a mathematical model for a rigid barrier with a ^{perfectly} absorbing edge is given by the canonical problem of diffraction by a semi-infinite rigid half-plane with a soft edge. We propose to solve this mixed boundary value problem.

In section one the canonical boundary value problem is formulated. In section two a solution is obtained for the formulated boundary value problem. The mathematical method used to solve the problem is Jones' method and the Wiener-Hopf technique, Noble [4]. Section three consists

We must now consider what we mean when we talk about a ^{perfectly} absorbing surface. The problem of mathematically describing a perfectly absorbing surface (or black surface) goes back to the last century. Such men as Kirchhoff, Kotler, Voigt and Macdonald were interested in this problem. A full discussion of the various theories is given in Baker and Copson's book "Mathematical theory of Huygens principle" Oxford 1949. The exact definition of a perfectly absorbing surface has never been satisfactorily resolved. One definition which seems to agree well with experimental measurements, has the disadvantage that it cannot be formulated as a mathematical boundary value problem. This definition of a perfectly absorbing surface is characterised as follows: Let an incident pressure wave $p_0 = \exp\{-ik(x\cos\theta_0 + y\sin\theta_0)\}$ be incident on a hard (rigid) surface $y=0, -\infty < x < \infty$. The total field (p_h) in $y > 0$ is given by

$$p_h = p_0, \quad x+y > 0,$$
$$= p_0 + \exp\{-ik(x\cos\theta_0 - y\sin\theta_0)\}, \quad x+y < 0.$$

Let the same wave p_0 be incident on a soft ^(pressure release) surface $y=0, -\infty < x < \infty$. The total field (p_s) in $y > 0$ is given by

$$p_s = p_0, \quad x+y > 0,$$
$$= p_0 - \exp\{-ik(x\cos\theta_0 - y\sin\theta_0)\}, \quad x+y < 0.$$

If the above two solutions p_h and p_s are added together and the result divided by two one obtains

$$p_A = \frac{1}{2}(p_s + p_h) = p_0, \quad -\infty < x < \infty, \quad y > 0.$$

This new solution which we have denoted by p_A has the property that the surface $y = 0, -\infty < x < \infty$ gives no reflected wave. Thus, it is as though all the energy of the incident wave is absorbed by the surface. However the solution p_A defies a mathematical boundary value problem formulation, or a physically mechanical construction. This definition does not depend on absorptive properties of the surface because it is supposed to be perfectly absorbing. As an upper bound to practical experimental work it is probably a useful yard stick.

of asymptotic expressions for the far field which are useful in obtaining graphs. These expressions are also conceptually easily related to the physical problem. Sections four and five are the graphical results and the conclusion drawn from them, respectively.

1. Formulation of the boundary value problem

A semi-infinite half-plane is assumed to occupy $y = 0, x \leq 0$; see figure 1. The half-plane is assumed to be infinitely thin, and over the interval $(-l, 0)$ to $(0, 0)$ a highly absorbing material is assumed to require the satisfaction of the soft boundary condition $p = 0$; and on the intervals $(-l, 0)$ to $(-\infty, 0)$ a rigid (hard) surface requires the satisfaction of the boundary condition $\partial p / \partial y = 0$ where p is the perturbation sound pressure. The perturbation velocity \underline{u} of the irrotational sound wave can be expressed in terms of a velocity potential $\chi(x, y)$ by $\underline{u} = \text{grad } \chi(x, y)$. The resulting pressure in the sound field is given by

$$p = -\rho_0 \frac{\partial \chi(x, y)}{\partial t},$$

where ρ_0 is the density of the ambient medium.

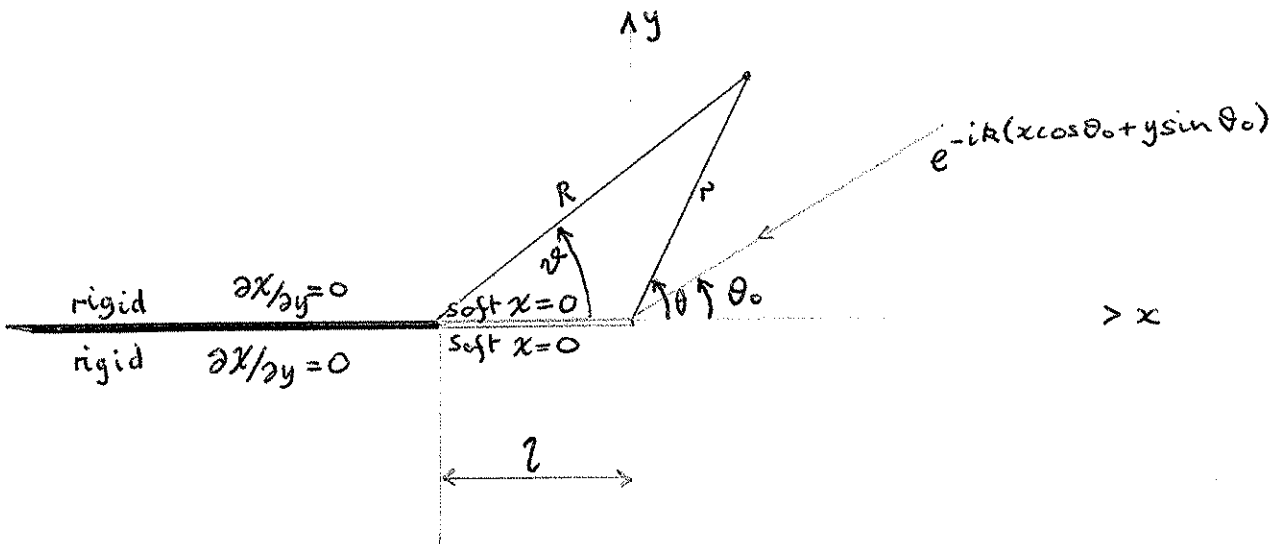


Figure 1

We shall assume that an incident plane wave sound field

$$\phi_0(x, y) = \exp\{-ik(x\cos\theta_0 + y\sin\theta_0) - i\omega t\},$$

$$0 < \theta_0 < \pi,$$
(1)

is diffracted by the half-plane. In future work we shall drop the time harmonic variation term $e^{-i\omega t}$. Then our problem becomes one of solving the wave equation

$$\left\{ \frac{\partial^2}{\partial x^2} + \frac{\partial^2}{\partial y^2} + k^2 \right\} \chi(x, y) = 0,$$
(2)

subject to the boundary conditions

$$\frac{\partial \chi(x, 0^+)}{\partial y} = 0, \quad x < -l,$$

$$\frac{\partial \chi(x, 0^-)}{\partial y} = 0;$$
(3)

$$\chi(x, 0^+) = 0, \quad -l < x < 0,$$

$$\chi(x, 0^-) = 0;$$
(4)

$$\chi(x, 0^+) = \chi(x, 0^-), \quad x > 0,$$

$$\frac{\partial \chi(x, 0^+)}{\partial y} = \frac{\partial \chi(x, 0^-)}{\partial y}.$$
(5)

We assume that a solution can be written in the following form

$$\chi(x, y) = \phi_0(x, y) + \phi(x, y),$$
(6)

where $\phi(x, y)$ represents the perturbed field due to the presence of the half-plane.

For analytic convenience we assume $k = k_r + ik_i$, ($k_r, k_i > 0$);

in which case for a unique solution of the boundary value problem (1) to (6) we also require the satisfaction of the radiation condition

$$\phi(x, y) = O\left(\frac{e^{-k_i r}}{\sqrt{r}}\right), \text{ as } r = \sqrt{(x^2 + y^2)} \rightarrow \infty; \quad (7)$$

and also the "edge condition" see Jones [5]

$$\chi(x, 0) = O(1), \text{ and } \frac{\partial \chi(x, 0)}{\partial y} = O(x^{-1/2}), \text{ as } x \rightarrow 0^+; \quad (8)$$

$$\chi(x, 0) = O(1), \text{ and } \frac{\partial \chi(x, 0)}{\partial y} = O((x+l)^{-1/2}), \text{ as } x \rightarrow -l.$$

2. Solution of the boundary value problem

We introduce the Fourier transform

$$\Phi(\alpha, y) = \int_{-\infty}^{\infty} \phi(x, y) e^{i\alpha x} dx, \quad (9)$$

and its inverse (if it exists)

$$\phi(x, y) = \frac{1}{2\pi} \int_{-\infty+i\tau}^{\infty+i\tau} \Phi(\alpha, y) e^{-i\alpha x} d\alpha, \quad (10)$$

where $\alpha = \sigma + i\tau$.

The transform (9) and its inverse (10)

will exist provided $-k_i < \tau < k_i \cos \theta_0$; this follows

from the radiation condition (7) and the form of the incident wave (1).

Applying (9) to the equation (2) gives

$$\Phi(\alpha, y) = A(\alpha) e^{i\kappa y}, \quad y > 0, \quad (11)$$

$$= B(\alpha) e^{-i\kappa y}, \quad y < 0; \quad (12)$$

where $\kappa = \sqrt{(k^2 - \alpha^2)}$ is defined on the cut sheet for which $\text{Im}(\kappa) > 0$ when $|\text{Im}(\alpha)| < k_i$. From the equations (11) and (12) we have

$$\begin{aligned} e^{-i\alpha l} \Phi_-(\alpha, 0^+) + \Phi_1(\alpha, 0^+) + \Phi_+(\alpha, 0) &= A(\alpha), \\ e^{-i\alpha l} \Phi'_-(\alpha, 0^+) + \Phi'_1(\alpha, 0^+) + \Phi'_+(\alpha, 0) &= i\kappa A(\alpha); \end{aligned} \quad (13)$$

$$\begin{aligned} e^{-i\alpha l} \Phi_-(\alpha, 0^-) + \Phi_1(\alpha, 0^-) + \Phi_+(\alpha, 0) &= B(\alpha), \\ e^{-i\alpha l} \Phi'_-(\alpha, 0^-) + \Phi'_1(\alpha, 0^-) + \Phi'_+(\alpha, 0) &= -i\kappa B(\alpha); \end{aligned} \quad (14)$$

where

$$\begin{aligned} \Phi_+(\alpha, y) &= \int_0^{\infty} \phi(x, y) e^{i\alpha x} dx, \\ \Phi_-(\alpha, y) &= \int_{-\infty}^{-l} \phi(x, y) e^{i\alpha(x+l)} dx, \\ \Phi_1(\alpha, y) &= \int_{-l}^0 \phi(x, y) e^{i\alpha x} dx. \end{aligned} \quad (15)$$

The primes denote differentiation with respect to y , and the \pm subscripts denote functions which are regular and analytic in the upper ($\text{Im}(\alpha) > -k_i$) and lower ($\text{Im}(\alpha) < k_i \cos \theta_0$) α -plane. Eliminating $A(\alpha)$ from (13) and $B(\alpha)$ from (14) yields the equations

$$\begin{aligned} e^{-i\alpha l} \Phi'_-(\alpha, 0^\pm) + \Phi'_1(\alpha, 0^\pm) + \Phi'_+(\alpha, 0) \\ = \pm i\kappa [e^{-i\alpha l} \Phi_-(\alpha, 0^\pm) + \Phi_1(\alpha, 0^\pm) + \Phi_+(\alpha, 0)]. \end{aligned}$$

(16a, b)

Applying the Fourier transform to the boundary condition (3) gives

$$\frac{\partial}{\partial y} \left\{ \int_{-\infty}^{-l} (\phi_0 + \phi) e^{i\alpha x} dx \right\}_{y=\pm 0} = 0$$

or

$$\Phi'_-(\alpha, 0^\pm) = \frac{k \sin \theta_0}{(\alpha - k \cos \theta_0)} e^{i k l \cos \theta_0} \quad (17)$$

Similarly the boundary condition (4) gives

$$\Phi_1(\alpha, 0^\pm) = \frac{i [1 - e^{-i(\alpha - k \cos \theta_0)l}]}{(\alpha - k \cos \theta_0)} \quad (18)$$

Substituting (17) and (18) into (16a, b) gives

$$\begin{aligned} & \frac{-k \sin \theta_0}{(\alpha - k \cos \theta_0)} e^{-i(\alpha - k \cos \theta_0)l} + \Phi'_1(\alpha, 0^\pm) + \Phi'_+(\alpha, 0) \\ &= \pm i \kappa \left[e^{-i\alpha l} \Phi_-(\alpha, 0^\pm) + \frac{i [1 - e^{-i(\alpha - k \cos \theta_0)l}]}{(\alpha - k \cos \theta_0)} \right] + \Phi'_+(\alpha, 0). \end{aligned}$$

(19a, b)

Adding and subtracting the equations (19a, b) gives

$$\begin{aligned} & -\frac{i \kappa e^{-i\alpha l}}{2} \left[\Phi_-(\alpha, 0^+) - \Phi_-(\alpha, 0^-) \right] + \frac{[\Phi'_1(\alpha, 0^+) + \Phi'_1(\alpha, 0^-)]}{2} + \Phi'_+(\alpha, 0) \\ &= \frac{-k \sin \theta_0}{(\alpha - k \cos \theta_0)} e^{-i(\alpha - k \cos \theta_0)l} \end{aligned} \quad (20)$$

$$\begin{aligned}
 & - e^{-i\alpha l} \frac{[\Phi_-(\alpha, 0^+) + \Phi_-(\alpha, 0^-)]}{2} + \frac{1}{i\kappa} \frac{[\Phi'_1(\alpha, 0^+) - \Phi'_1(\alpha, 0^-)]}{2} - \Phi_+(\alpha, 0) \\
 & = i \frac{[1 - e^{-i(\alpha - k \cos \theta_0)l}]}{(\alpha - k \cos \theta_0)}.
 \end{aligned} \tag{21}$$

The equations (20) and (21) can be written in the more convenient forms

$$\mathcal{N}_-(\alpha) + e^{i\alpha l} \mathcal{N}_+(\alpha) = - \frac{k \sin \theta_0 e^{ikl \cos \theta_0}}{\sqrt{(k+\alpha)(\alpha - k \cos \theta_0)}}, \tag{22}$$

$$e^{-i\alpha l} \mathcal{Y}_-(\alpha) + L(\alpha) \mathcal{Y}_1(\alpha) + \mathcal{Y}_+(\alpha) = \frac{i [e^{-i(\alpha - k \cos \theta_0)l} - 1]}{(\alpha - k \cos \theta_0)}, \tag{23}$$

where

$$\begin{aligned}
 \mathcal{N}_-(\alpha) &= \frac{\sqrt{(k-\alpha)}}{2i} [\Phi_-(\alpha, 0^+) - \Phi_-(\alpha, 0^-)], \\
 \mathcal{N}_+(\alpha) &= \frac{1}{\sqrt{(k+\alpha)}} \left\{ \frac{[\Phi'_1(\alpha, 0^+) + \Phi'_1(\alpha, 0^-)]}{2} + \Phi'_+(\alpha, 0) \right\}, \tag{24}
 \end{aligned}$$

$$\mathcal{Y}_-(\alpha) = \frac{[\Phi_-(\alpha, 0^+) + \Phi_-(\alpha, 0^-)]}{2},$$

$$\mathcal{Y}_1(\alpha) = i \frac{[\Phi'_1(\alpha, 0^+) - \Phi'_1(\alpha, 0^-)]}{2},$$

$$\Psi_+(\alpha) = \Phi_+(\alpha, 0),$$

$$L(\alpha) = (k^2 - \alpha^2)^{-1/2}, \quad L(\alpha) = L_+(\alpha)L_-(\alpha),$$

$$L_{\pm}(\alpha) = (k \pm \alpha)^{-1/2}.$$

Before we proceed further with equations (22) and (23) we shall require to know how the various quantities in (24) grow as $|\alpha| \rightarrow \infty$.

The edge condition (8) means that the transformed functions satisfy the following as $|\alpha| \rightarrow \infty$

$$\Phi_+(\alpha) \sim O(|\alpha|^{-1}), \quad \Phi'_+(\alpha) \sim O(|\alpha|^{-1/2}), \quad \text{in } \text{Im}(\alpha) > -k_i;$$

$$\Phi_-(\alpha) \sim O(|\alpha|^{-1}), \quad \Phi'_-(\alpha) \sim O(|\alpha|^{-1/2}), \quad \text{in } \text{Im}(\alpha) < k_i \cos \theta_0;$$

$$e^{i\alpha l} \Phi_{,1}(\alpha) \sim O(|\alpha|^{-1}), \quad e^{i\alpha l} \Phi'_{,1}(\alpha) \sim O(|\alpha|^{-1/2}), \quad \text{in } \text{Im}(\alpha) > -k_i;$$

$$\Phi_{,1}(\alpha) \sim O(|\alpha|^{-1}), \quad \Phi'_{,1}(\alpha) \sim O(|\alpha|^{-1/2}), \quad \text{in } \text{Im}(\alpha) < k_i \cos \theta_0. \quad (26)$$

Using the asymptotic estimates (26), in the expressions (24), we have, as $|\alpha| \rightarrow \infty$,

$$\sqrt{L}_-(\alpha) \sim O(|\alpha|^{-1/2}), \quad \Psi_-(\alpha) \sim O(|\alpha|^{-1}), \quad \Psi_{,1}(\alpha) \sim O(|\alpha|^{-1/2})$$

$$L_-(\alpha) = O(|\alpha|^{-1/2}), \quad \text{in } \text{Im}(\alpha) < k_i \cos \theta_0; \quad (27)$$

$$\sqrt{L}_+(\alpha) \sim O(|\alpha|^{-1}), \quad \Psi_+(\alpha) \sim O(|\alpha|^{-1}), \quad \Psi_{,1}(\alpha) \sim O(e^{-i\alpha l} |\alpha|^{-1/2}),$$

$$L_+(\alpha) \sim O(|\alpha|^{-1/2}), \quad \text{in } \text{Im}(\alpha) > -k_i. \quad (28)$$

The equation (22) can be written in the form

$$\begin{aligned} \sqrt{V}_-(\alpha) + \frac{k \sin \theta_0 e^{ikl \cos \theta_0}}{\sqrt{(k+k \cos \theta_0)(\alpha - k \cos \theta_0)}} &= \\ = - e^{i\alpha l} \sqrt{V}_+(\alpha) - \frac{k \sin \theta_0}{(\alpha - k \cos \theta_0)} \left\{ \frac{1}{\sqrt{(k+\alpha)}} - \frac{1}{\sqrt{(k+k \cos \theta_0)}} \right\} e^{ikl \cos \theta_0}, \end{aligned} \quad (29)$$

where the left-hand side of the equality sign is regular, analytic and asymptotic to $|\alpha|^{-1/2}$ as $|\alpha| \rightarrow \infty$ in the region $\text{Im}(\alpha) < k i \cos \theta_0$; and the right-hand side of the equality sign is regular, analytic, and asymptotic to $|\alpha|^{-1}$ as $|\alpha| \rightarrow \infty$ in the half-plane $\text{Im}(\alpha) > -ki$.

Hence by the usual Wiener-Hopf argument, Noble [4] the analytic function which is a continuation of the left-hand side and the right-hand side of equation (29) in the whole α -plane is zero. Thus

$$\sqrt{V}_-(\alpha) = - \frac{k \sin \theta_0 e^{ikl \cos \theta_0}}{\sqrt{(k+k \cos \theta_0)(\alpha - k \cos \theta_0)}},$$

or

$$\Phi_-(\alpha, 0^+) - \Phi_-(\alpha, 0^-) = \frac{-2i \sqrt{(k - k \cos \theta_0)} e^{ikl \cos \theta_0}}{\sqrt{(k-\alpha)(\alpha - k \cos \theta_0)}}. \quad (30)$$

The equation (23) cannot be split by the standard Wiener-Hopf argument because of the second term on the left-hand side. However, it can be shown that equation (23) can be put in an equivalent form in terms of Fredholm integral equations of the second kind. Without going through the details, which in any case can be found, Mutatis Mutandis, in Noble [4], pp. 196-199, we obtain

$$S_+^*(\alpha) = \frac{i\sqrt{(k+k\cos\theta_0)}}{\sqrt{(k+\alpha)(\alpha-k\cos\theta_0)}} + \frac{1}{2\pi i\sqrt{(k+\alpha)}} \int_{-\alpha+ia}^{\alpha+ia} \frac{e^{i\zeta^2} \sqrt{(k-\zeta)} S_+^*(\zeta)}{(\zeta+\alpha)} d\zeta,$$

$$-\text{Im}(\alpha) < a < k\cos\theta_0,$$

$$D_+^*(\alpha) = \frac{i\sqrt{(k+k\cos\theta_0)}}{\sqrt{(k+\alpha)(\alpha-k\cos\theta_0)}} - \frac{1}{2\pi i\sqrt{(k+\alpha)}} \int_{-\alpha+ia}^{\alpha+ia} \frac{e^{i\zeta^2} \sqrt{(k-\zeta)} D_+^*(\zeta)}{(\zeta+\alpha)} d\zeta,$$

$$-\text{Im}(\alpha) < a < k\cos\theta_0,$$

(31)

(32)

where

$$S_+^*(\alpha) = \underline{Y}_+(\alpha) + \underline{Y}_-(-\alpha) + \frac{i}{(\alpha - k\cos\theta_0)} + \frac{i e^{ikl\cos\theta_0}}{(\alpha + k\cos\theta_0)},$$

(33)

$$D_+^*(\alpha) = \underline{Y}_+(\alpha) - \underline{Y}_-(-\alpha) + \frac{i}{(\alpha - k\cos\theta_0)} - \frac{i e^{ikl\cos\theta_0}}{(\alpha + k\cos\theta_0)},$$

(34)

The asterisks denote that a pole is present at $\alpha = k\cos\theta_0$ in the region $\text{Im}(\alpha) > -k\cos\theta_0$, otherwise the functions are regular and analytic in this domain.

An exact solution of the equations (31) and (32) would be too difficult to obtain. We therefore obtain an approximate asymptotic solution for the situation where $kl \gg 1$. The physical meaning of this condition is that the soft tip covers a region greater than a wavelength.

In the expression (31) the path of integration is moved vertically so that it crosses the pole $\alpha = k \cos \theta_0$ of $S_+^*(\alpha)$. However the path is not allowed to cross the branch point $\alpha = k$. Thus the third term of (33) will give a residue contribution so that

$$S_+^*(\alpha) = \frac{i \sqrt{(k+k \cos \theta_0)}}{\sqrt{(k+\alpha)(\alpha-k \cos \theta_0)}} + \frac{i \sqrt{(k-k \cos \theta_0)} e^{ikl \cos \theta_0}}{\sqrt{(k+\alpha)(\alpha+k \cos \theta_0)}} + \frac{1}{2\pi i \sqrt{(k+\alpha)}} \int_{-\infty+ia}^{\infty+ia} \frac{e^{i\zeta l} \sqrt{(k-\zeta)} S_+^*(\zeta)}{(\zeta+\alpha)} d\zeta$$

(35)

$$k \cos \theta_0 < \alpha < k$$

Since $kl \gg 1$ the dominant term of the asymptotic expansion for the integral appearing in (35) comes from the region near $\zeta = k$ so that

$$\frac{1}{2\pi i} \int_{-\infty+ia}^{\infty+ia} \frac{e^{i\zeta l} \sqrt{(k-\zeta)} S_+^*(\zeta)}{(\zeta+\alpha)} d\zeta \approx \frac{S_+^*(k)}{2\pi i} \int_{-\infty+ia}^{\infty+ia} \frac{e^{i\zeta l} \sqrt{(k-\zeta)}}{(\zeta+\alpha)} d\zeta (1+R)$$

where $R = \frac{1}{2kl(1-\cos \theta_0)} + O\left(\frac{1}{(kl)^2}\right)$ (36)

provided $S_+^*(k)$ is well behaved in this region, which it will be provided

$\theta_0 \neq 0, \pi$. The integral (36) can now be evaluated by wrapping the contour of integration around the branch cut $\zeta = k$.

It can then be shown that

$$\begin{aligned} \frac{1}{2\pi i} \int_{-\infty+ia}^{\infty+ia} \frac{e^{i\zeta l} \sqrt{(k-\zeta)}}{(\zeta+\alpha)} &= \frac{e^{ikl}}{\pi} \int_0^{\infty} \frac{e^{i\eta t} t^{1/2}}{(t+k+\alpha)} dt, \quad \text{Im}(\alpha) > -a, \\ &= \frac{e^{i(kl+\pi/4)}}{\sqrt{\pi l}} \left\{ 1 + 2i \sqrt{(k+\alpha)l} F(\sqrt{(k+\alpha)l}) \right\}, \\ &\quad l > 0, \quad |\arg(k+\alpha)| < \pi, \\ &= W_0[\sqrt{(k+\alpha)l}], \end{aligned}$$

(37)

where $F(z) = e^{-iz^2} \int_z^{\infty} e^{it^2} dt,$

is the Fresnel integral. Hence on substituting the above results into (35) we obtain

$$\begin{aligned} S_+^*(\alpha) &= \frac{i\sqrt{(k+k\cos\theta_0)}}{\sqrt{(k+\alpha)(\alpha-k\cos\theta_0)}} + \frac{i\sqrt{(k-k\cos\theta_0)} e^{ikl\cos\theta_0}}{\sqrt{(k+\alpha)(\alpha+k\cos\theta_0)}} \\ &\quad + \frac{S_+^*(k)}{\sqrt{(k+\alpha)}} W_0[\sqrt{(k+\alpha)l}]. \end{aligned}$$

(38)

The term $S_+^*(k)$ can be obtained by letting $\alpha = k$ in (38) and solving for $S_+^*(k)$.

By a completely analogous method the equation (32) gives

$$D_+^*(\alpha) = \frac{i \sqrt{(k + k \cos \theta_0)}}{\sqrt{(k + \alpha)(\alpha - k \cos \theta_0)}} - \frac{i \sqrt{(k - k \cos \theta_0)} e^{ikl \cos \theta_0}}{\sqrt{(k + \alpha)(\alpha + k \cos \theta_0)}} \\ - \frac{D_+^*(k) W_0 [\sqrt{(k + \alpha)l}]}{\sqrt{(k + \alpha)}}$$

(39)

where $D_+^*(k)$ is obtained by putting $\alpha = k$ in the above expression and solving for $D_+^*(k)$. Expressions (38) and (40), on being substituted into (33) and (34), give expressions for $Y_{\pm}(\alpha)$, from which, in conjunction with (24) and (30) produce expressions for $\Phi_+(\alpha, 0)$, $\Phi_-(\alpha, 0^{\pm})$. Substituting these latter expressions together, with (18), into the first equations of (13) and (14) gives:

$$A(\alpha) = \frac{i}{(\alpha - k \cos \theta_0)} \left\{ \frac{\sqrt{(k + k \cos \theta_0)}}{\sqrt{(k + \alpha)}} - \frac{2 \sqrt{(k - k \cos \theta_0)} e^{-i(\alpha - k \cos \theta_0)l}}{\sqrt{(k - \alpha)}} \right\} \\ + \frac{W_0 [\sqrt{(k + \alpha)l}]}{2 \sqrt{(k + \alpha)}} \{ S_+^*(k) - D_+^*(k) \} \\ + e^{-i\alpha l} \frac{W_0 [\sqrt{(k - \alpha)l}]}{2 \sqrt{(k - \alpha)}} \{ S_+^*(k) + D_+^*(k) \},$$

(40)

$$\begin{aligned}
 B(\alpha) = & \frac{i\sqrt{(k+k\cos\theta_0)}}{\sqrt{(k+\alpha)(\alpha-k\cos\theta_0)}} + \frac{W_0[\sqrt{(k+\alpha)\tau}]}{2\sqrt{(k+\alpha)}} \{S_+^*(k) - D_+^*(k)\} \\
 & + e^{-i\alpha\tau} \frac{W_0[\sqrt{(k-\alpha)\tau}]}{2\sqrt{(k-\alpha)}} \{S_+^*(k) + D_+^*(k)\}.
 \end{aligned}
 \tag{41}$$

The solution to the boundary problem is now known and is given by

$$\chi(x,y) = \phi_0(x,y) + \frac{1}{2\pi} \int_{-\infty+i\tau}^{\infty+i\tau} A(\alpha) e^{-i\alpha x + i\kappa y} d\alpha, \quad y > 0,$$

(42)

$$= \phi_0(x,y) + \frac{1}{2\pi} \int_{-\infty+i\tau}^{\infty+i\tau} B(\alpha) e^{-i\alpha x - i\kappa y} d\alpha, \quad y < 0,$$

(43)

$$-ki < \tau < k\cos\theta_0.$$

3. Asymptotic expressions for the far field

For the purposes of plotting the polar diagram of the scattered far field the expressions (42) and (43) are asymptotically evaluated for kr large. The results below can be obtained by an application of the saddle point method, modified slightly because of the presence of the pole $\alpha = k\cos\theta_0$, see Jones [5] or Rawlins [3].

Thus, for $0 < \theta_0 < \pi$, without going through the detailed

analysis, one obtains

$$\begin{aligned}
 \chi(r, \theta) &= I + RF + D_1, & \text{for } \pi - \theta_0 < \vartheta < \pi, \\
 &= I - RF + D_1, & \text{for } \vartheta < \pi - \theta_0 < \theta, \\
 &= I + D_1, & \text{for } 0 < \theta < \pi - \theta_0, \\
 &= I + D_2, & \text{for } \theta_0 - \pi < \theta < 0, \\
 &= D_2, & \text{for } -\pi < \theta < \theta_0 - \pi;
 \end{aligned}$$

(44)

where $x = r \cos \theta$, $y = r \sin \theta$, $-\pi \leq \theta \leq \pi$,

and incident plane wave $= I = e^{-ikr \cos(\theta - \theta_0)}$,

reflected wave $= RF = e^{-ikr \cos(\theta + \theta_0)}$

Diffracted edge wave in the illuminated region $= D_1$

$$\begin{aligned}
 D_1 &= - \frac{e^{i(kr - \pi/4)}}{\sqrt{(2\pi kr)}} \cdot \frac{2|Q|F(|Q|)}{(\cos \theta + \cos \theta_0)} \cdot \sqrt{(1 + \cos \theta)} \sqrt{(1 + \cos \theta_0)} \\
 &+ \frac{e^{i(kR - \pi/4)}}{\sqrt{(2\pi kR)}} \cdot \frac{2|Q'|F(|Q'|)}{(\cos \vartheta + \cos \theta_0)} \cdot 2\sqrt{(1 - \cos \vartheta)} \sqrt{(1 - \cos \theta_0)} e^{ikl \cos \theta_0} \\
 &+ \frac{e^{i(kr - \pi/4)}}{\sqrt{(2\pi kr)}} \cdot G_1(\theta, \theta_0) + \frac{e^{i(kR - \pi/4)}}{\sqrt{(2\pi kR)}} \cdot G_2(\vartheta, \theta_0),
 \end{aligned}$$

Diffracted edge wave in the shadow region = D_2

$$D_2 = - \frac{e^{i(kr - \pi/4)}}{\sqrt{(2\pi kr)}} \cdot \frac{2|Q|F(|Q|)}{(\cos\theta + \cos\theta_0)} \cdot \sqrt{(1 + \cos\theta)}\sqrt{(1 + \cos\theta_0)}$$

$$+ \frac{e^{i(kr - \pi/4)}}{\sqrt{(2\pi kr)}} G_1(\theta, \theta_0) + \frac{e^{i(kR - \pi/4)}}{\sqrt{(2\pi kR)}} G_2(\vartheta, \theta_0).$$

In D_1 and D_2 the various quantities appearing are given by

$$Q = \sqrt{\frac{k\Gamma}{2}} \cdot \left(\frac{\cos\theta + \cos\theta_0}{\sin\theta} \right), \quad Q' = \sqrt{\frac{kR}{2}} \cdot \left(\frac{\cos\vartheta + \cos\theta_0}{\sin\vartheta} \right),$$

$$R^2 = r^2 + l^2 + 2rl\cos\theta, \quad \vartheta = \text{sgn}(\theta) \cdot \cos^{-1}\left(\frac{l + r\cos\theta}{R}\right),$$

$$G_1(\theta, \theta_0) = \frac{W_0 [\sqrt{k}l(1 - \cos\theta)]}{\sqrt{2k}} \cdot \left\{ \frac{k}{\sqrt{2}} (S_+^*(k) - D_+^*(k)) \right\} \sqrt{(1 + \cos\theta)},$$

$$G_2(\vartheta, \theta_0) = \frac{W_0 [\sqrt{k}l(1 + \cos\vartheta)]}{\sqrt{2k}} \cdot \left\{ \frac{k}{\sqrt{2}} (S_+^*(k) + D_+^*(k)) \right\} \sqrt{(1 - \cos\vartheta)},$$

and
$$F(|z|) = e^{-iz^2} \int_{|z|}^{\infty} e^{it^2} dt,$$

which is the Fresnel integral. For large z the Fresnel integral can be replaced by the dominant term of its asymptotic series i.e.

$$F(|z|) \sim \frac{i}{2|z|} + O(|z|^{-3}), \quad \text{as } |z| \rightarrow \infty$$

$|\arg z| < \pi.$

From the first expression of (44) it will be noticed that the sign of the reflected wave corresponds to reflection from the rigid part of the barrier. In the second expression of (44) the reflected wave sign corresponds to reflection from the soft region of the barrier.

Butler [1] has observed that ^{the solution for} the perfectly absorbing semi-infinite plane agrees well with the experimental results of Maekawa [6] on absorbing barriers. ^{solution} The perfectly absorbing semi-infinite plane _A is given by adding the hard and soft semi-infinite plane solutions and dividing by two. Naturally the same incident wave is used in the hard and soft half plane solutions. The same technique can be used in the present work. By simply adding the solution for a hard half plane, say $\phi_h(x, y)$, to $\chi(x, y)$ and dividing by two the solution for a perfectly absorbing strip of length $(-l < x < 0)$ connected to a hard plane $(-\infty < x < -l)$ is given, say $\chi_A(x, y) (= (\phi_h(x, y) + \chi(x, y))/2)$. $\phi_h(x, y)$ satisfies the conditions (1), (2), (5), (6), and the boundary conditions (3) and (4) are replaced by $\partial \phi_h(x, 0^\pm) / \partial y = 0, (x < 0)$. The appropriate explicit solution for $\phi_h(x, y)$ is given in Noble [4]. The equivalent expressions to (41), (42) and (44) for a perfectly absorbing strip are given by

$$A_A(\alpha) = \left\{ A(\alpha) - i \sqrt{(k - k \cos \theta_0) / (\alpha - k \cos \theta_0)} \sqrt{(k - \alpha)} \right\} / 2 \quad (45)$$

$$B_A(\alpha) = \left\{ B(\alpha) + i \sqrt{(k - k \cos \theta_0) / (\alpha - k \cos \theta_0)} \sqrt{(k - \alpha)} \right\} / 2 ;$$

$$\begin{aligned}
 \chi_A(r, \theta) &= I + RF + D_1 + D_3, & \text{for } \pi - \theta_0 < \theta < \pi, \\
 &= I + D_1 + D_3, & \text{for } 0 < \theta < \pi - \theta_0, \\
 &= I + D_2 - D_3, & \text{for } \theta_0 - \pi < \theta < 0, \\
 &= D_2 - D_3, & \text{for } -\pi < \theta < \theta_0 - \pi,
 \end{aligned}
 \tag{46}$$

where

$$D_3 = \frac{e^{i(kr - \pi/4)}}{\sqrt{2\pi kr}} \cdot \frac{2|Q|F(|Q|)}{2(\cos\theta + \cos\theta_0)} \cdot \sqrt{(1 - \cos\theta)}\sqrt{(1 - \cos\theta_0)}.$$

It will be noticed that the reflected wave from the absorbent strip region has disappeared.

4. Graphical results

The expressions (44) and (46) were used to give graphical polar plots of the modulus of the far field i.e. $|\chi(r, \theta)|$, $|\chi_A(r, \theta)|$, for $kr = 10\pi$. The values of kl that were chosen were $0, 2\pi, 5\pi, 15\pi$ and ∞ . The case of $kl = 0$ and $kl = \infty$ correspond to the completely hard and completely soft/perfectly absorbing semi-infinite plane

solutions respectively. These polar diagrams are given in graphs (1) to (9) for an angle of incidence of $\theta_0 = 90^\circ$. Graph (10) is the attenuation of the sound field, i.e. $20 \log_{10} |\chi(r, \theta)|$, in the shadow region of a hard screen with a soft strip for $\theta_0 = 90^\circ$, and $kl = 0, \pi, 2\pi, \infty$.

Graph (11) is the attenuation of the sound field, i.e. $20 \log_{10} |\chi_A(r, \theta)|$ in the shadow region of a hard screen with a perfectly absorbing strip for $\theta_0 = 90^\circ$, and $kl = 2\pi, \infty$.

For the purpose of comparison the attenuation for a completely hard semi-infinite plane is also shown in graphs (10) and (11). The graphs for $kl = 0$ are given by the hard half plane solution $\phi_h(x, y)$, given in Noble [4].

From the graphs (10) and (11) it can be seen that the attenuation in the shadow region of the screen is very insensitive to the quantity kl , which is related to the width of the strip and the wave length of the sound. Provided that $kl > 1$ the field in the shadow region is, to all

intents and purposes, the same as that for $k\ell = \infty$. The difference in attenuation between the soft and hard half plane is greater than that between the perfectly absorbing and hard half plane. The sound field level and orientation on the illuminated side of the screen is more acutely affected by the quantity $k\ell$. However, it can be seen from graphs (1) to (9) that provided $k\ell > 15\pi$ the sound field in the illuminated region is approximately the same as that for $k\ell = \infty$.

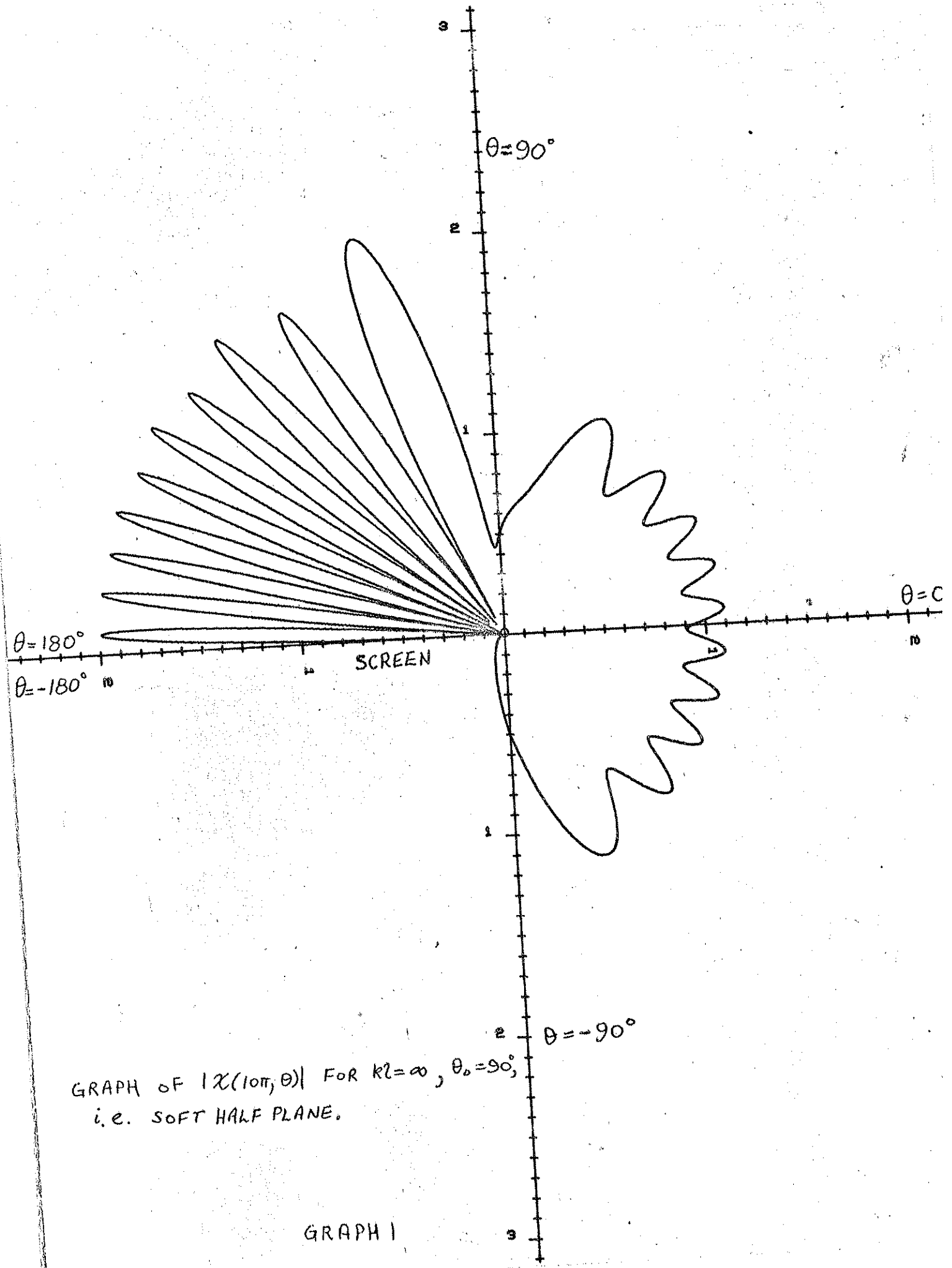
Conclusions

From the graphical results we may infer that most of the increased attenuation, in the shadow region, which is predicted for a completely absorbent screen over a rigid screen is obtainable by applying sound absorbent material to within a wave length of the edge of a rigid screen. Some recent experimental work by Butler [6] would seem to fully support this inference.

The magnitude of attenuation in the shadow region for the soft strip problem is much more than one would expect to achieve in practice with an absorbing strip. However, this is to be expected because no practical surface is entirely soft. Closer agreement with experimental measurements, for an absorbing strip, is probably given by the attenuation graphs for a perfectly absorbing strip.

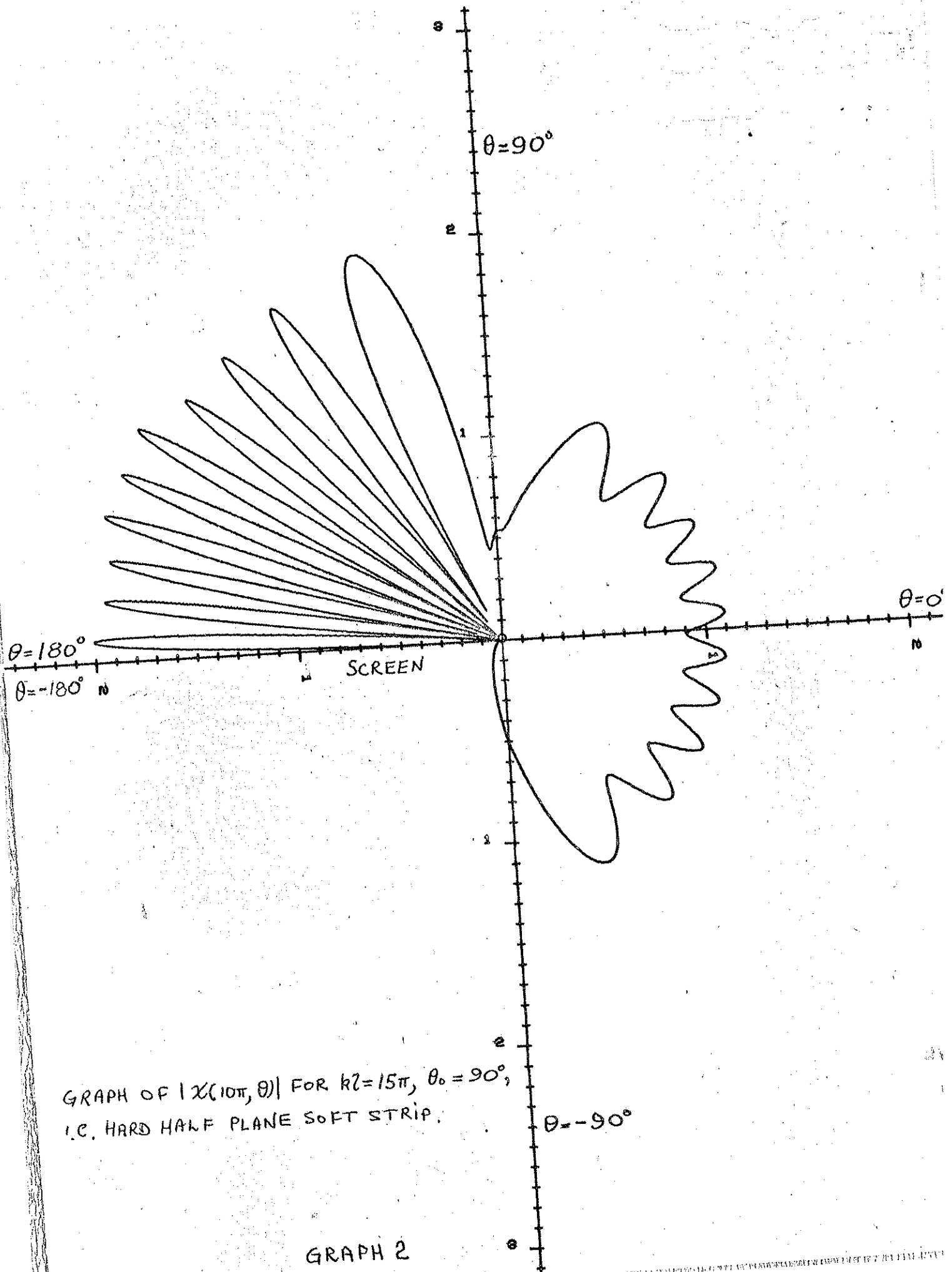
The orientation and magnitude of the far field on the source side of the semi-infinite plane seems to depend more critically on $k\ell$. This is due to the constructive/destructive interaction of the edge diffracted fields with the reflected wave from the hard region $-\infty < x < -\ell$, and the reflected wave from the region $-\ell < x < 0$. The attenuation of the far field, in this half space, will probably be greatly affected by the absorptive properties of the strip. For

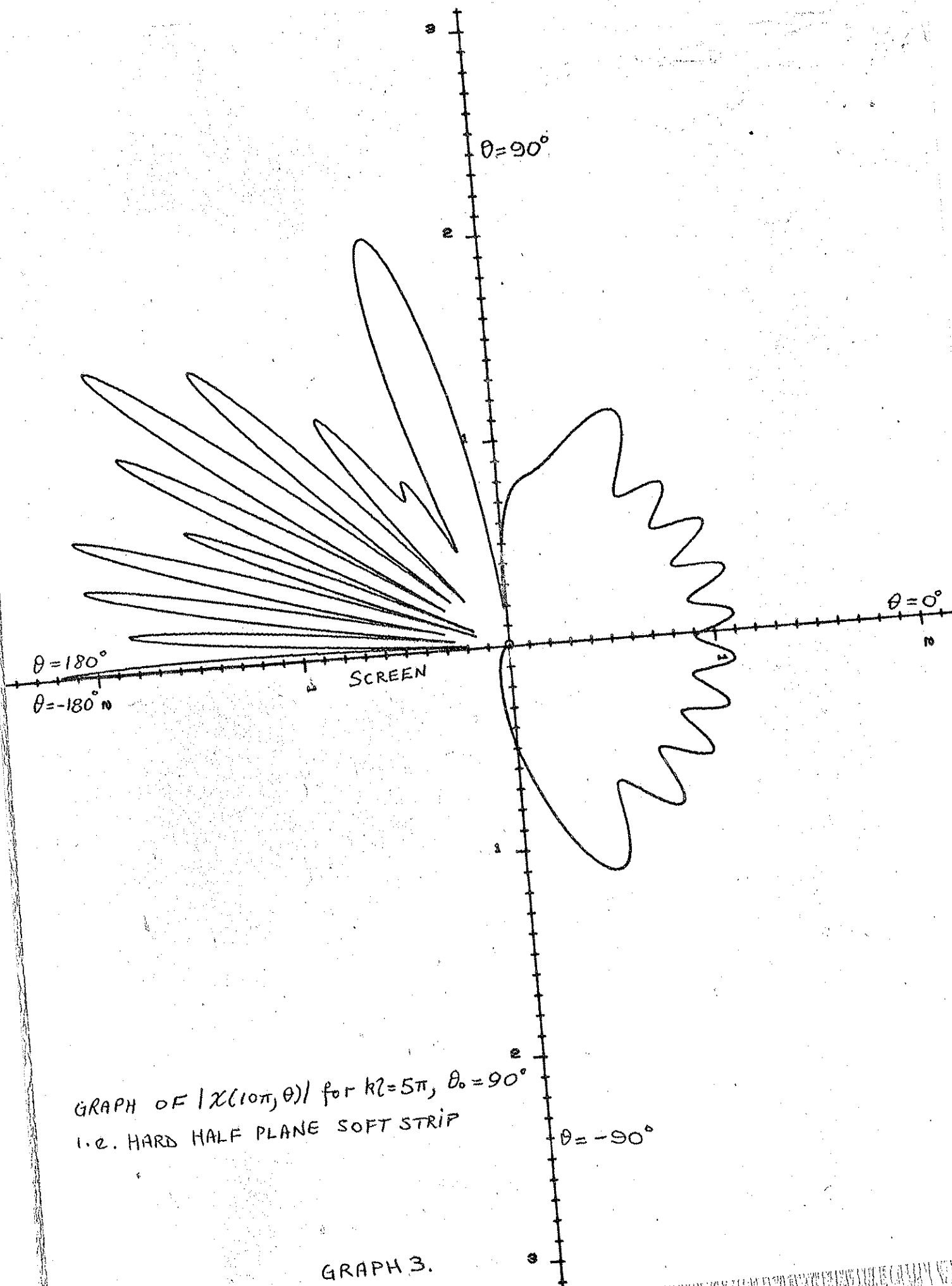
instance, in the second expression of (44) the reflected wave term will be multiplied by a Fresnel reflection coefficient. This Fresnel coefficient, which will be a function of the angle of incidence and the absorptive parameter of the strip, could vanish for certain value of these variables. In such a situation the far field would be considerably reduced. A more detailed analysis of the field in this region will appear in a forthcoming publication, in which a solution is given for the more general problem of a strip with an impedance boundary condition connected to a rigid semi-infinite plane.



GRAPH OF $|\chi(10\pi, \theta)|$ FOR $kl = \infty$, $\theta_0 = 90^\circ$,
 i.e. SOFT HALF PLANE.

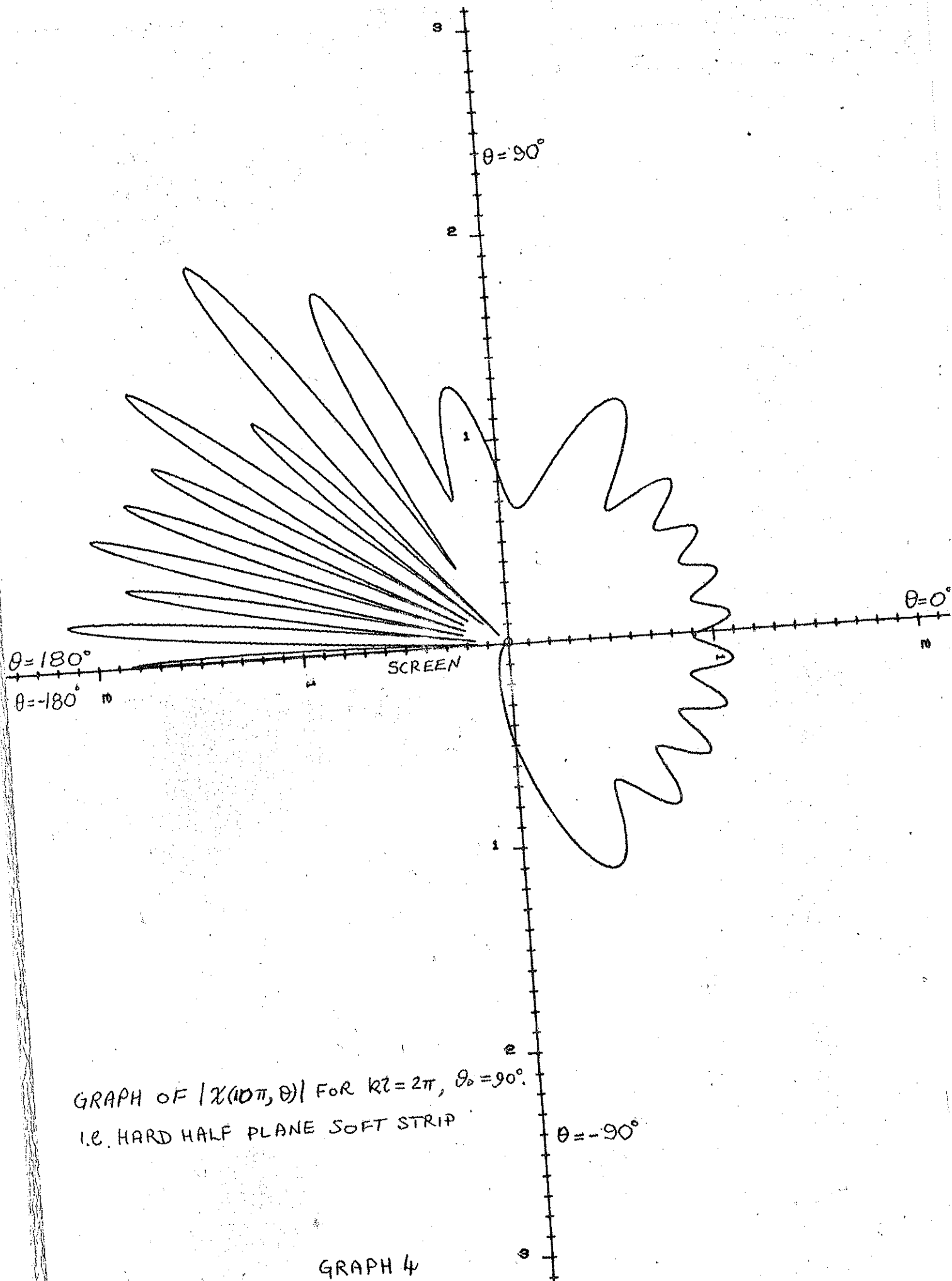
GRAPH 1





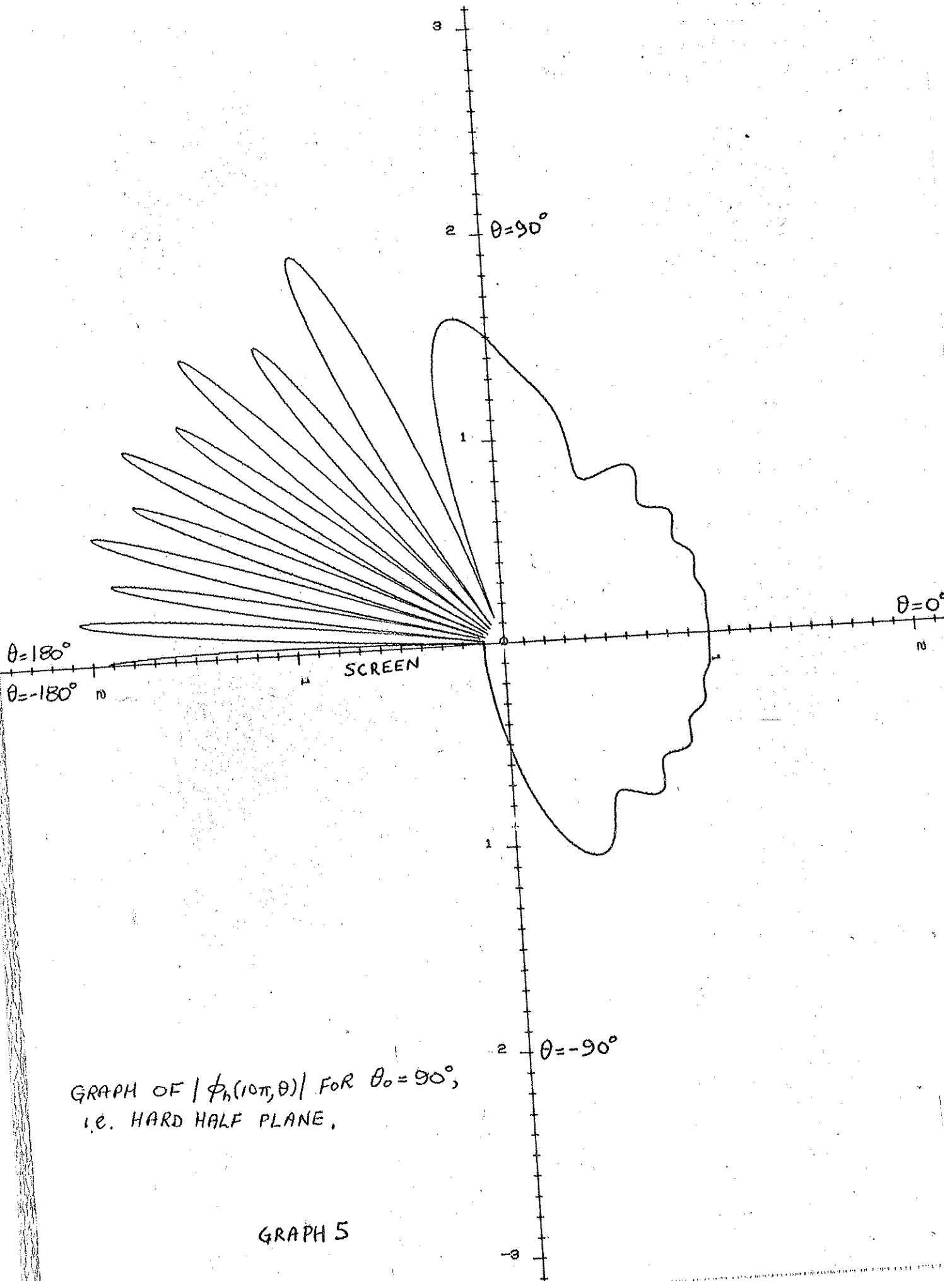
GRAPH OF $|\chi(10\pi, \theta)|$ FOR $k\ell = 5\pi$, $\theta_0 = 90^\circ$
 I.E. HARD HALF PLANE SOFT STRIP

GRAPH 3.



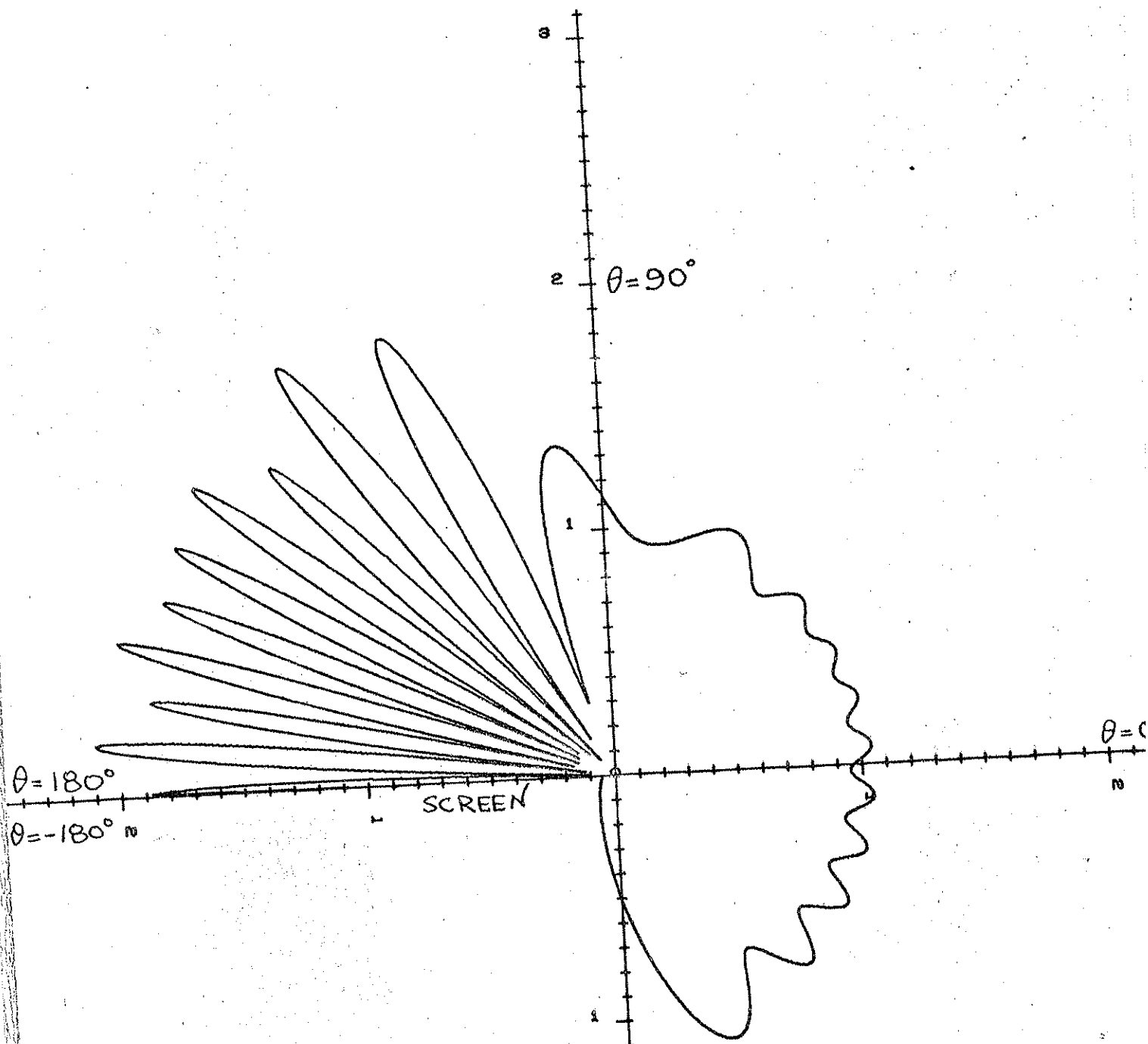
GRAPH OF $|\chi(10\pi, \theta)|$ FOR $kz = 2\pi$, $\theta_0 = 90^\circ$.
 I.E. HARD HALF PLANE SOFT STRIP

GRAPH 4



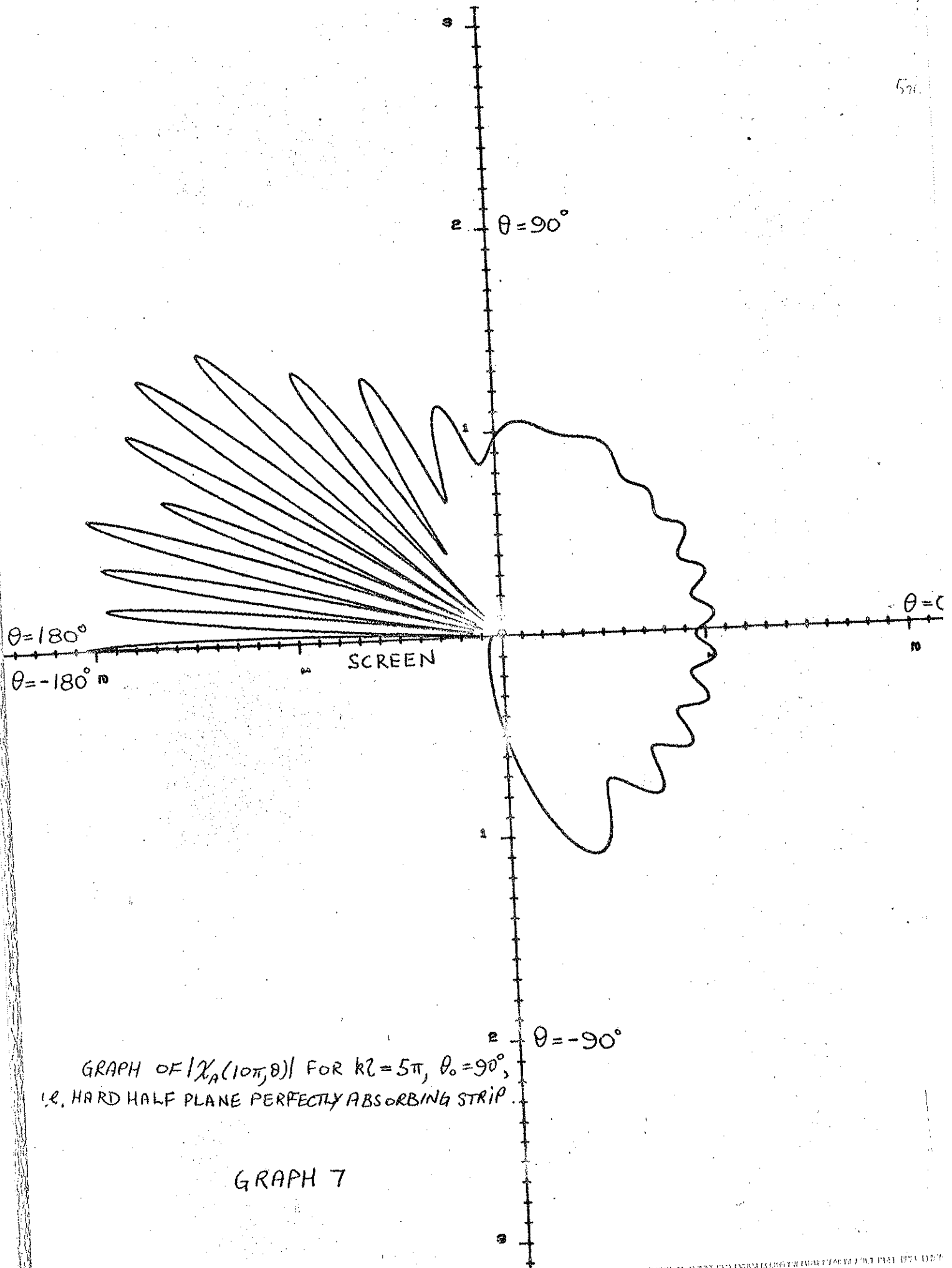
GRAPH OF $|\phi_h(10\pi, \theta)|$ FOR $\theta_0 = 90^\circ$,
 I.E. HARD HALF PLANE,

GRAPH 5



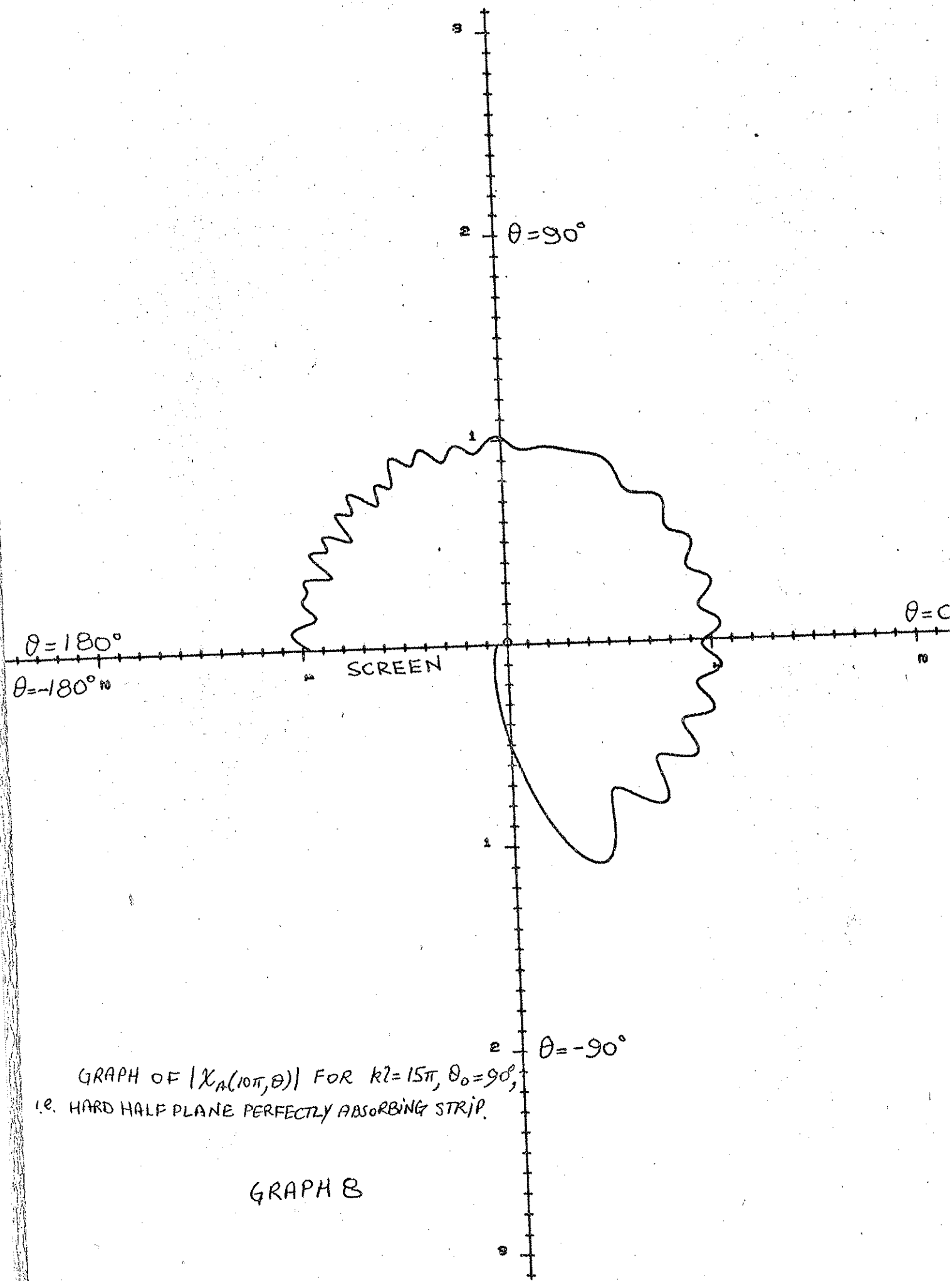
GRAPH OF $|\chi_R(10\pi, \theta)|$ FOR $k_2 = 2\pi$, $\theta_0 = 90^\circ$,
 (R. HARD HALF PLANE PERFECTLY ABSORBING STRIP.)

GRAPH 6.



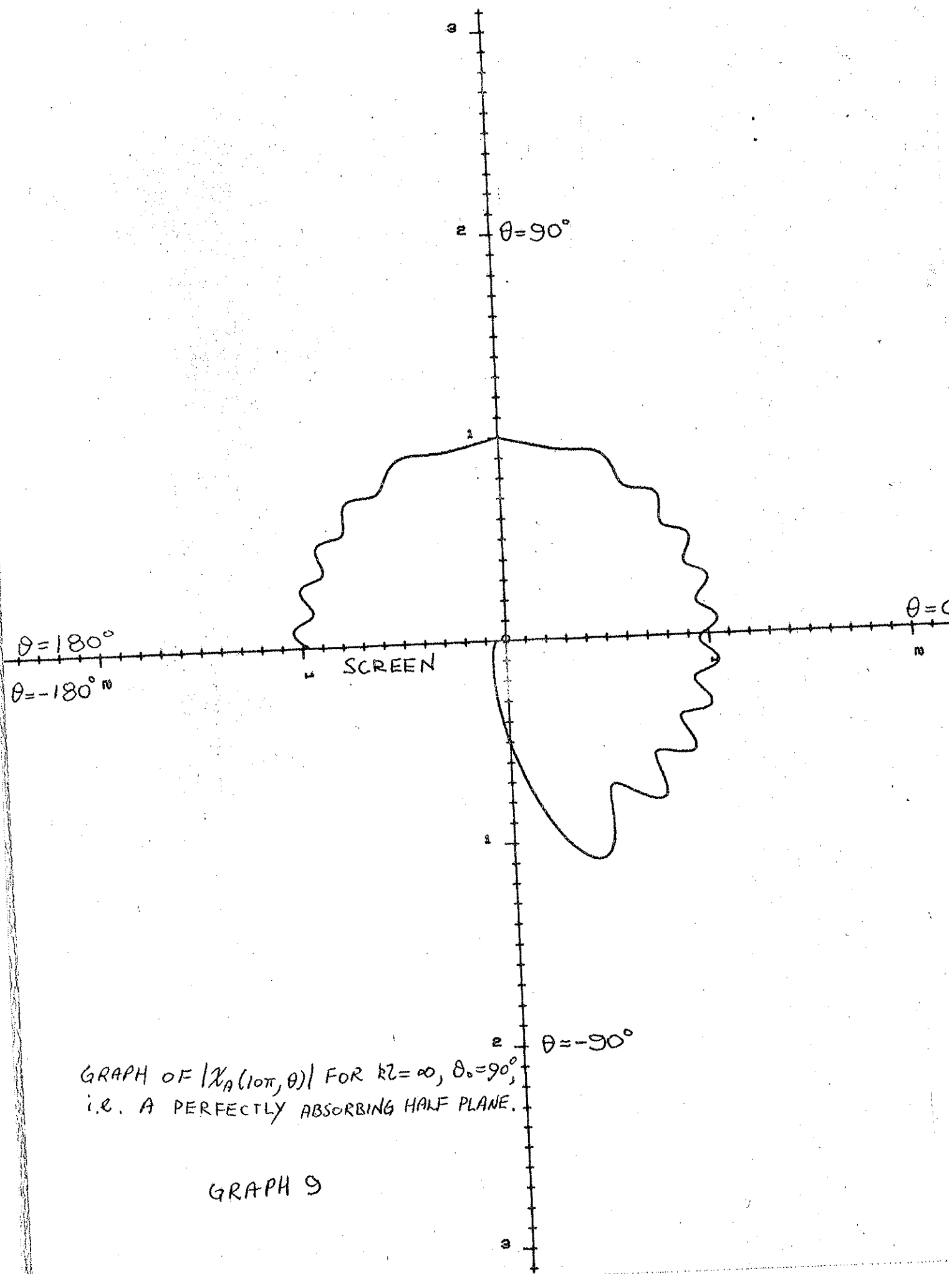
GRAPH OF $|\chi_A(10\pi, \theta)|$ FOR $kL = 5\pi$, $\theta_0 = 90^\circ$,
I.E. HARD HALF PLANE PERFECTLY ABSORBING STRIP.

GRAPH 7



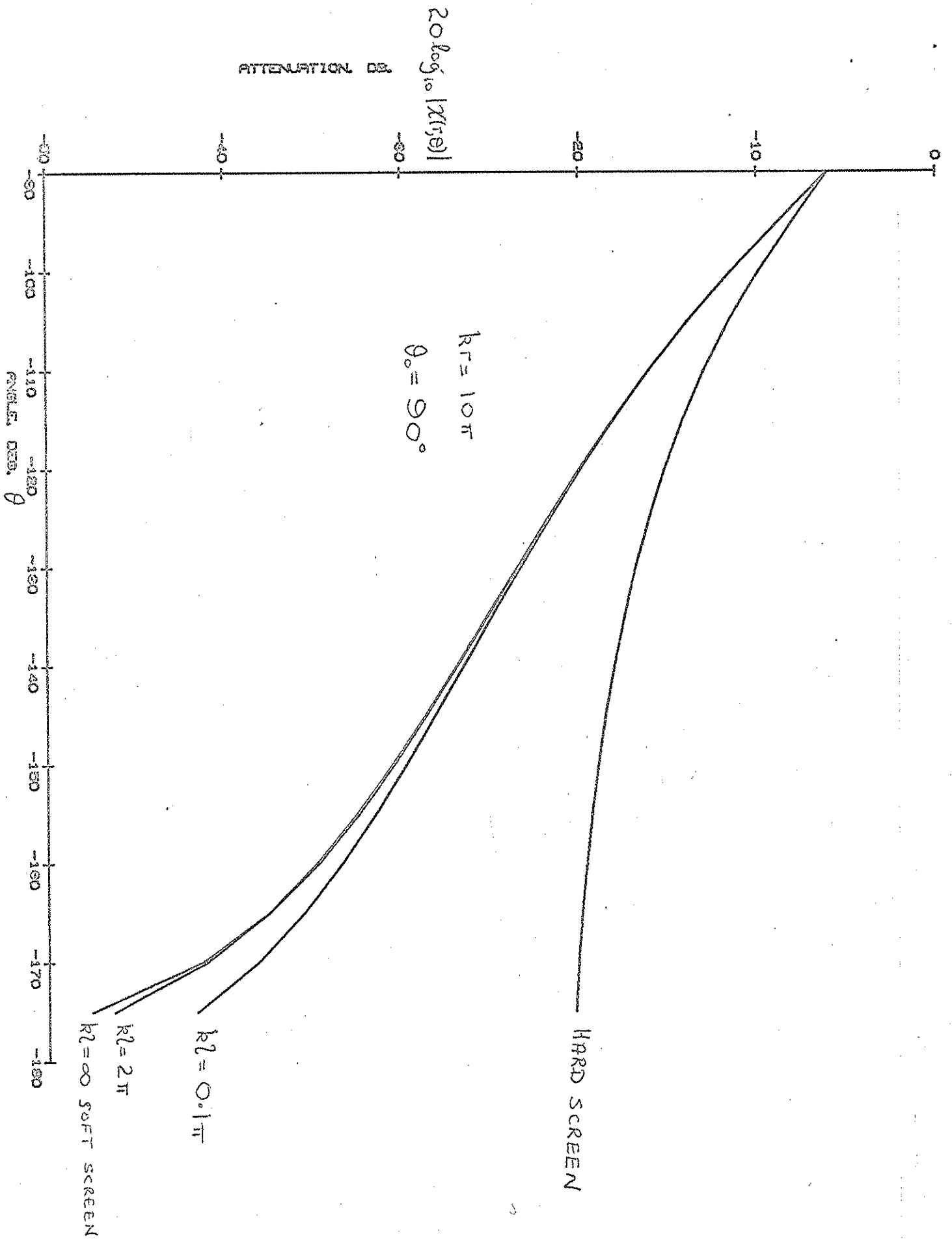
GRAPH OF $|\chi_A(10\pi, \theta)|$ FOR $k^2 = 15\pi$, $\theta_0 = 90^\circ$,
 i.e. HARD HALF PLANE PERFECTLY ABSORBING STRIP.

GRAPH B



GRAPH OF $|\chi_A(10\pi, \theta)|$ FOR $k_2 = \infty$, $\theta_0 = 90^\circ$,
 i.e. A PERFECTLY ABSORBING HALF PLANE.

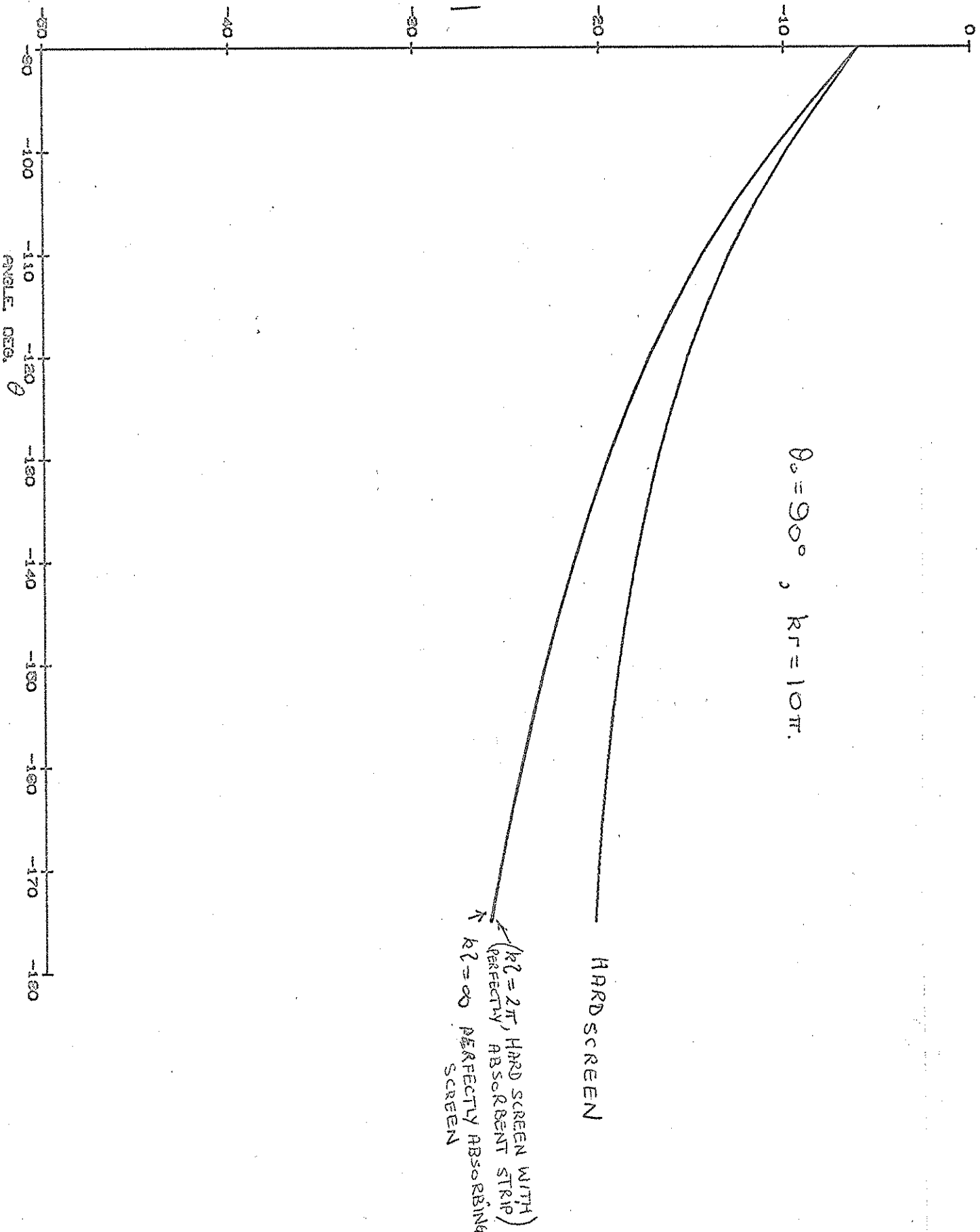
GRAPH 9



GRAPH 10

20 log₁₀ |R₂₁|

ATTENUATION, DB.



GRAPH 11

Sray

R E F E R E N C E S

1. G. F. Butler, Journal of Sound and Vibration, 32, (1974), pp. 367-369.
2. P. M. Morse and K. U. Ingard, Encyclopedia of Phys, Acoustics I, Springer Verlag, (1961).
3. A. D. Rawlins, Proc. Roy. Soc. Edin., A72 1974, pp. 337-357
4. B. Noble, The Wiener-Hopf technique, Pergamon, (1958).
5. D. S. Jones, The thoery of **E**lectromagnetism, Pergamon, (1964).
6. Z. Maekawa, Noise reduction by screens, Memoirs of Faculty of Engineering, Kobe University. No. 11, (1965) pp. 29-53.